The interaction of error fields and resistive wall modes

C. G. Gimblett and R. J. Hastie
EURATOM/UKAEA Fusion Association, Culham Science Centre, Abingdon, Oxon, OX 14 3DB, United Kingdom

(Received 7 July 2003; accepted 12 November 2003)

An investigation is presented of the effect of an error field on the growth of a resistive wall mode (RWM). This issue is of importance to many toroidal confinement devices, but particularly to the proposed International Thermonuclear Experimental Reactor (ITER) [ITER Physics Basis, Nucl. Fusion **39**, 2175 (1999)], where if advanced tokamak performance is required, then the RWM instability is especially vulnerable. The paper includes a discussion of error field amplification when RWM marginal stability is approached, and it is pointed out that error field current is the fixed quantity in this calculation, *not* the error field flux, which is essentially an eigenvalue of the calculation. The key issue concerns the effect of plasma rotation on the RWM. The distinction is made between the resistive wall *tearing* mode (RWTM), which is stabilized by modest plasma rotation, and the ideal RWM, which is not. The importance of the joint torques that are present when an error field and an RWM of the same helicity coexist is investigated. Using torque balance a simulation is presented of the effect of reducing error field amplitude on the duration of a stable discharge. This shows features in accord with experimental observations from the DIII-D device [J. L. Luxon *et al.*, *Plasma Physics and Controlled Fusion Research* (International Atomic Energy Agency, Vienna, 1987), Vol. 1, p.159]. [DOI: 10.1063/1.1639155]

I. INTRODUCTION

It is now generally accepted that advanced tokamak (AT) equilibria, such as might be envisaged for the operation of the International Thermonuclear Experimental Reactor (ITER),[1] require wall stabilization in order to achieve optimized central shear and produce economically attractive β limits.[2,3] A desirable target is that the AT should reach the magnetohydrodynamic (MHD) β stability limits that are predicted when the surrounding wall is considered as ideally conducting.[4] However, if the finite resistivity of the wall is taken into account, the resistive wall mode (RWM) is predicted to be destabilized.[5] This mode is a relevant concern for many toroidal plasma confinement devices[6,7] but the AT will be particularly vulnerable to it, as the presence of a largely uniform current density profile in the central core implies that the external kink version of the RWM can readily be activated.

In a previous publication[8] we investigated the nonlinear evolution of an RWM in a cylindrical tokamak model[9] when the RWM stability threshold is exceeded. This would occur in a toroidal equilibrium when the no-wall β-limit is surpassed. The plasma model included toroidal plasma rotation and an internal mode rational surface at which dissipative effects (such as plasma resistivity[10] and/or viscosity[11]) become important and thereby introduce nonideal MHD effects into the plasma dynamics of an RWM. It was found that, as the RWM grows in amplitude, it exerted an increasing torque on the plasma, and so accordingly reduced the natural plasma rotation. Since the RWM linear stability threshold may itself be a function of the plasma rotation, one possible outcome was that a nonlinear saturation of the RWM might occur as the rotation decreased. This, however, required that (a) a window of RWM stability existed (for $\Omega_1<\Omega<\Omega_2$, where Ω is the toroidal plasma rotation at the internal resonant surface) and that the initial plasma rotation exceeded the upper boundary, $\Omega>\Omega_2$. Other possibilities are that (b) plasma rotation ($\Omega\neq 0$) merely reduces linear growth rates, but never eliminates the RWM entirely, or that (c) linear RWM stability requires sufficiently rapid rotation ($\Omega>\Omega_3$). In these two latter cases, after the onset of an RWM, the nonlinear torque exerted by the mode reduces the plasma rotation, Ω, leading to an acceleration of the RWM growth rate.

The difficulty of making reliable predictions of RWM behavior lies in the fact that different models of the dissipation mechanism within the plasma lead to differing linear RWM stability thresholds as functions of Ω. In previous work[8] we found that with inertial-resistive[10] layer physics a narrow stability window in Ω does exist for the RWM [case (a) above], but only if the RWM is very weakly unstable in a stationary plasma. In the presence of strong perpendicular viscous drag in the resonant layer[11] the RWM is not stabilized by any sub-Alfvénic plasma rotation [case (b) above]. Earlier work[12,13] investigated the effects of continuum damping and found stability above a critical rotation frequency [case (c) behavior].

As a result of these calculations it was concluded in Ref. 8 that the RWM should become unstable as soon as the no-wall β-limit is exceeded and that, after onset of the RWM, one should observe a slowing down of the plasma rotation and accelerating growth of the mode. In particular it was predicted that the plasma rotation should display a sudden flip to a lower value when Ω fell to some critical value (the

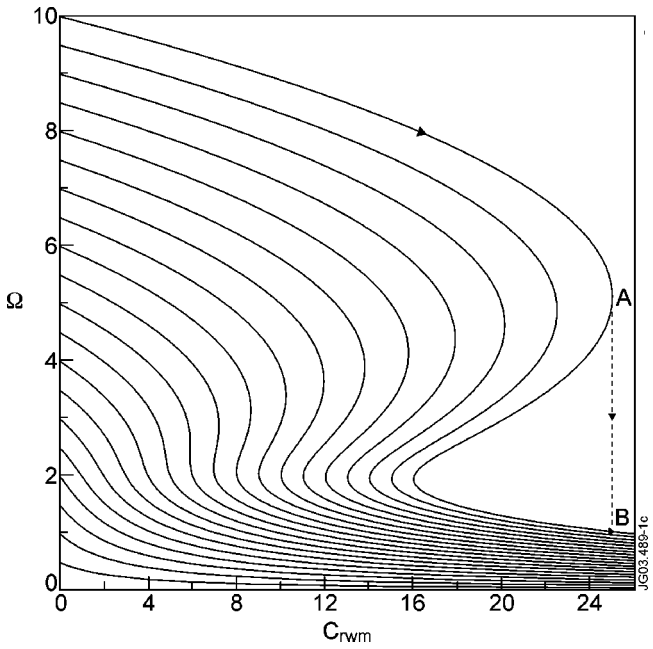

FIG. 1. Equilibrium *S*-curves in the absence of an error field. Plasma rotation rate $\Omega\tau_w$ against RWM amplitude, constructed from Eq. (38) with $\epsilon = 0.01$, $\delta = 0.5$, $\tau_L/\tau_w = 1$.

so-called *S*-curve, Fig. 1) accompanied by more rapid RWM growth.

Experimental observations on the DIII-D tokamak[14] (see Fig. 2) reported this type of behavior. However, although the qualitative predictions of the theory appeared to be correct, the parameters (rotation rates, mode amplitudes, etc.) observed experimentally[15,16] did not seem to accord with those of Ref. 8. In addition it was observed that the period of very weak growth of the RWM could be greatly prolonged in

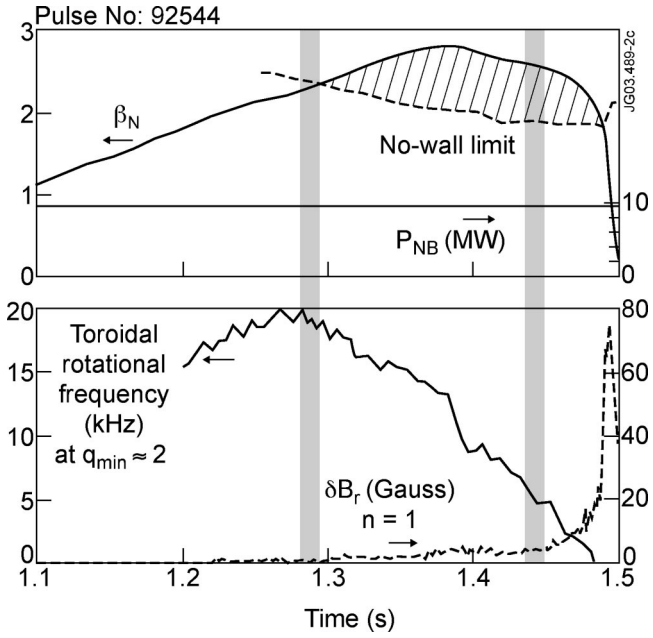

FIG. 2. Experimental results from DIII-D. The top graph shows β_N relative to the no-wall β limit. The lower graph shows the toroidal rotation rate at the $q=2$ surface and the magnitude of the RWM magnetic perturbation.

DIII-D[17] by careful reduction of stationary error fields. This observation has lead to renewed theoretical interest in the influence of error fields on RWM stability. In particular Fitzpatrick[18] and Boozer[19] have recently published the results of such investigations.

Since these authors draw somewhat different conclusions to those which we draw in this paper, we begin by describing the assumptions and results of these papers.

II. A REVIEW OF RECENT RESULTS CONCERNING THE RWM AND ERROR FIELDS

Boozer[19] focuses on the external circuitry required to identify the resonant component of the error fields and to cancel this by generating suitable additional perturbations. Here the term resonant means those error fields containing the same mix of poloidal and toroidal harmonics as the natural eigenmode of the RWM. To identify this mix, one must either calculate it (requiring the correct choice of plasma model and computation in realistic toroidal geometry) or measure it. The difficulty of the calculational approach lies in the fact that ideal MHD codes are inadequate for this purpose. The correct departures from ideal MHD must be included. Boozer therefore assumes that the resonant component is known by direct experimental measurement of the RWM fluctuations just outside the plasma boundary. The Boozer interpretation of the DIII-D observations is as follows: Suppose that, whatever the nonideal internal plasma dynamics might be, it is such that the RWM can be stabilized for a sufficiently large plasma rotation [case (c) noted above]. Suppose also that there is a finite resonant error field. This is effectively generated by the presence of some small helical current perturbations in external field coils (e.g., by small coil misalignments). Although these helical current perturbations are fixed (i.e., not time dependent), the resulting magnetic field perturbations at the plasma boundary and within the plasma are not. They are functions of the evolving tokamak equilibrium and they increase as the RWM stability boundary is approached. The resulting torque exerted by the error fields also increases as the RWM stability threshold is approached, and this, in turn, leads to a slowing down of the plasma rotation. Thus, although the initial plasma rotation may have been sufficient to stabilize the RWM, $\Omega_0 > \Omega_3$, the magnification of the error fields and their torque can cause Ω to fall below the critical value, Ω_3, with the result that, when the RWM threshold (for a stationary plasma) is crossed, the RWM instability begins to grow. In Boozer's picture the DIII-D results display this behavior. Boozer argues that case (c) above is probably generic and that reduction of the resonant error field to negligible magnitude and maintenance of a moderate value of the plasma rotation, Ω, will eliminate RWM instability. At this point it is worth noting that the DIII-D data[14] (see the bottom trace of Fig. 2) do not unambiguously support this interpretation. In Fig. 2 the spin-down of the plasma rotation does not appear to precede the onset of the RWM, and the RWM appears to grow as soon as the no-wall β-limit is crossed, even though the rotation frequency has the high value of $f = \Omega(r_s)/(2\pi) \sim 20$ kHz.

Fitzpatrick[18] employs a specific, cylindrical plasma

model (the Fitzpatrick–Aydemir model[20]) and calculates the effect of error fields within this model. The Fitzpatrick–Aydemir model includes plasma rotation, but contains no internal mode rational surface effects. The essential nonideal plasma dynamics appears instead in a strongly visco-inertial layer at the plasma-vacuum boundary. Mathematically this region performs a similar role to the internal mode rational surface in the Finn model.[9] However, whereas in the Finn model the Δ' jump through the layer is proportional to $(\gamma + i\Omega(r_s))\tau_L$ the jump through the Fitzpatrick–Aydemir boundary layer is proportional to $(\gamma+i\Omega(a))(\tau_{A*}^2/\tau_\mu) + [(\gamma+i\Omega(a))\tau_{A*}]^2$, where γ is the complex growth rate, τ_L is a time characteristic of the layer at the mode rational surface, $r=r_s$, $\tau_\mu = a^2\rho(a)/\mu(a)$ is a viscous time and τ_{A*} is related to the Alfvén time with, typically, $\tau_{A*} \gg \tau_A$. This small difference in the respective layer physics leads to case (c) behavior for RWM stability in the Fitzpatrick–Aydemir model, but case (b) behavior for the Finn model with a visco-resistive layer. In addition, since the error field and RWM can only exert a torque on the plasma in regions of nonideal MHD plasma dynamics, the torques in the Fitzpatrick–Aydemir model appear only at the plasma edge. So finite edge rotation must be assumed. In the Finn model torques appear internally at the mode rational surface and we assume that edge recycling maintains a nearly stationary edge plasma (a no-slip boundary condition).

In this paper we employ the Finn model with visco-resistive layer physics to describe the plasma dynamics and calculate the magnitude of the electromagnetic torques ($T \propto \tilde{j}\times\tilde{b}$) exerted by a resonant error field and by a growing RWM. These torques are then used in the toroidal momentum equation to calculate the resulting reduction in the plasma rotation at the internal mode rational surface. There is a synergistic effect between the torques. Both torques act so as to reduce the rotation, $\Omega(r_s)$, and this reduction in Ω increases the magnitude of each torque.

III. RWM DISPERSION RELATION IN THE FINN MODEL

The dispersion relation for single helicity tearing modes and resistive wall modes in a cylindrical equilibrium surrounded by a resistive wall takes the form

$$\Delta_L(p) = \frac{\Delta'_\infty(1+\lambda\Delta'_w\Delta_w(p))}{1+\lambda\Delta'_\infty\Delta_w(p)}, \tag{1}$$

where the quantities Δ'_∞ and Δ'_w are the conventional tearing stability indices, calculated with no conducting wall and with a perfectly conducting wall at the location of the actual resistive wall (both quantities are real). The quantities $\Delta_L(p)$ and $\Delta_w(p)$ are the corresponding jumps across the internal resonant surface and through the resistive wall, respectively. They are functions of the complex mode growth rate, p, and are complex quantities. Throughout this paper we take the thin wall approximation for $\Delta_w(p)$,

$$\Delta_w(p) = p\tau_w, \tag{2}$$

where $\tau_w = r_w d/\eta_w$ is the wall diffusion time. d is the thickness of the wall, r_w and η_w its radius and resistivity. In Eq. (1) the factor λ depends on details of the equilibrium current profile, location of the persistive wall, and the poloidal mode number m. It can be absorbed into the definition of the wall time by writing $\lambda\tau_w \to \tau_w$. In the following discussions, however, we take $\%l = 1$ for simplicity. For the jump through the resonant layer we adopt the visco-resistive plasma model,[11]

$$\Delta_L(p) = (p+i\Omega)\tau_L, \tag{3}$$

where Ω is the toroidal rotation frequency of the plasma at the mode resonant surface, and τ_L is a characteristic layer time. We have assumed that the toroidal mode number $n=1$ for simplicity.

In the absence of the resistive wall [e.g., with $\Delta_w(p) \equiv 0$] this dispersion relation predicts an unstable tearing mode whenever $\Delta'_\infty > 0$ and an ideal MHD kink instability when $\Delta'_\infty \to \infty$. In the presence of the resistive wall the tearing mode is readily stabilized by plasma rotation, while the ideal MHD kink mode is converted to the resistive wall mode, with much slower growth rate, but is never completely stabilized by rotation. This is an example of case (b) behavior described in the introduction.

The resistive wall tearing mode (RWTM) occurs when $\Delta'_\infty > 0$ and $\Delta'_w < 0$ and is stabilized by plasma rotation,

$$\Omega\tau_L > \frac{\tau_L/\tau_w - \Delta'_\infty\Delta'_w}{\sqrt{-\Delta'_\infty\Delta'_w}}. \tag{4}$$

In a real tokamak equilibrium, as β_N (Ref. 14) increases under auxiliary heating the quantities Δ'_∞ and Δ'_w both increase, first passing through zero (tearing marginality), then tending to $+\infty$ (ideal MHD marginality). As Δ'_∞ passes through zero the RWTM becomes transiently unstable, but is quickly stabilized by plasma rotation as Δ'_∞ increases to $O(\tau_L/\tau_w) \ll 1$. However the RWTM stability criterion must again be violated at higher β, either because $\Delta'_\infty \to \infty$ (the ideal MHD no-wall β limit) or because $\Delta'_w \to 0$ from below (marginality of the tearing mode in the presence of a perfectly conducting wall). In practice it is not known which of these thresholds will occur first. The ideal MHD, no-wall, threshold is readily calculated with codes such as PEST or DCON, but the β limits for tearing modes are not known. Consequently, most previous interpretation of the experimental DIII-D data has focused on the RWM and, latterly, on the interaction of error fields with the plasma rotation and with the RWM. We will also follow this path here, but we note in passing that the DIII-D data may also be interpreted in terms of the RWTM.

In line with our previous notation[8] it is convenient to replace the quantities Δ'_∞ and Δ'_w by $-1/\epsilon$ and $-\delta$, respectively. ϵ is then a measure of the Alfvénic growth rate of the no-wall ideal MHD kink mode, and $\delta > 0$ corresponds to stability of tearing modes with a perfectly conducting wall at the location of the real wall. Using this notation and substituting Eqs. (2) and (3) into Eq. (1), one obtains a dispersion relation for the RWM and RWTM in the form

$$(p+i\Omega)\tau_L = \frac{1-\delta p\tau_w}{-\epsilon + p\tau_w}. \tag{5}$$

In what follows we will be particularly interested in the amplification of the error fields as ϵ approaches zero from the stable side, and in calculating the effect of the combined error field and RWM torques when $\epsilon>0$ and the RWM begins to grow.

IV. ERROR FIELD AMPLIFICATION IN THE FINN MODEL

Penetration of an error field into the plasma is also governed by the RWM dispersion [Eq. (5)], with the same visco-resistive layer response [the same $\Delta_L(p+i\Omega)$, with $p=0$]. However, the quantity $\Delta_w(p)$ must now be replaced by a jump condition across the field perturbing coil. Integrating radially across a helical current sheet we find

$$\Delta_{\mathrm{coil}}=-imI/\psi_E, \tag{6}$$

where I is a measure of the helical current responsible for the field error, m is the poloidal mode number and ψ_E is the helical flux at the coil location. The quantity ψ_E is itself a function of the plasma equilibrium (i.e., of ϵ and δ), while I is a true measure of the field error. With these changes, the RWM dispersion relation can now be solved as an eigenvalue problem. However, the complex eigenvalue is now ψ_E, the amplitude and phase of the error field at the location of the misaligned coil. Throughout the rest of the paper we will assume that the location of the error producing current I is coincident with that of the resistive wall at $r=r_w$.

Solution of the error field eigenvalue equation

$$i\Omega\tau_L=\frac{1+imI\delta/\psi_E}{-\epsilon-imI/\psi_E}, \tag{7}$$

yields the result

$$\frac{\psi_E}{\psi_{\mathrm{vac}}}=-2m\frac{\delta+i\Omega\tau_L}{1+i\Omega\tau_L\epsilon}, \tag{8}$$

so that

$$\left|\frac{\psi_E}{\psi_{\mathrm{vac}}}\right|=2m\left[\frac{\delta^2+\Omega^2\tau_L^2}{1+\Omega^2\tau_L^2\epsilon^2}\right]^{1/2}, \tag{9}$$

where, following Fitzpatrick,[18] we have replaced the error field current, I, by the resulting error field flux that would be produced at the coil in the absence of plasma, $\psi_{\mathrm{vac}}=iI/2$. Equation (9) quantifies error field amplification (or suppression) for the Finn model with visco-resistive plasma dynamics at the mode rational surface. In the limit of strong plasma rotation, $\Omega\tau_L\gg1$, there is strong error field amplification as $\epsilon\to0$, i.e., as β_N approaches the no-wall β limit. While in the limit of weak plasma rotation, $\Omega\tau_L\ll1$, error field amplification occurs only at higher values of β_N, where $\delta\to-\infty$, i.e., at the β limit for kink modes in the presence of a perfectly conducting wall. We note here that in Ref. 19 this distinction is not made. In the Fitzpatrick–Aydemir[20] model error field amplification occurs approaching the no-wall β limit.

V. ELECTROMAGNETIC TORQUES

In this section we calculate the torques in the toroidal direction exerted by a growing resistive wall instability and by the resonant component of the error field. These torques vanish in any region of the plasma where ideal MHD equations govern the plasma dynamics.[18] They therefore appear as delta function torques at the internal mode rational surface where we assume that linear visco-resistive physics determines the plasma response. The local toroidal electromagnetic torque is given by

$$T_\phi=\int rR^2\,dr\,d\theta\,d\phi(\tilde{j}\times\tilde{b}), \tag{10}$$

where $\tilde{j}$ and $\tilde{b}$ are the perturbed current density and magnetic field, respectively. Now representing $\tilde{b}$ in terms of real quantities as

$$\begin{aligned}\tilde{b}_r&=e^{\gamma t}b_r(r)\cos(\xi+\alpha),\\ \tilde{b}_\theta&=e^{\gamma t}(b_{\theta c}(r)\cos(\xi+\alpha)+b_{\theta s}(r)\sin(\xi+\alpha)),\\ \tilde{b}_\phi&=e^{\gamma t}(b_{\phi c}(r)\cos(\xi+\alpha)+b_{\phi s}(r)\sin(\xi+\alpha)),\end{aligned} \tag{11}$$

where $\xi=(m\theta-n\phi-\omega t)$, $\alpha(r)$ is a phase factor and where γ and ω are the growth rate and frequency of the RWM perturbations, zero for the error field. Denoting the error field perturbations as $\hat{b}_r$, $\hat{b}_{\theta c,s}$, etc., we calculate the torque directly to obtain

$$\begin{aligned}T_\phi(r)&=\int rR^2\,dr\,d\theta\,d\phi[\hat{j}\times\hat{b}+j\times b+\hat{j}\times b+j\times\hat{b}]\\ &=2\pi^2R_0^2\int r\,dr\Bigg[\frac{1}{r}\frac{d}{dr}(r\hat{b}_r\hat{b}_{\phi c})\\ &\quad+e^{2\gamma t}\frac{1}{r}\frac{d}{dr}(rb_rb_{\phi c})+\cos(\alpha-\hat{\alpha}-\omega t)\\ &\quad\times e^{\gamma t}(\hat{b}b)\mathrm{terms}\Bigg].\end{aligned} \tag{12}$$

For a slowly growing RWM the oscillatory cross coupling terms time average to zero, so we ignore them in what follows. Next, making use of $\nabla\cdot b=0$ and $[j_r]=0$ where $[Y]=Y(r_s+)-Y(r_s-)$, the torque takes the form

$$T_\phi=2\pi^2R_0^2r_sb_r^2e^{2\gamma t}\frac{kr_s}{m^2+k^2r_s^2}[r_s\alpha'], \tag{13}$$

with $k=n/R_0$. In terms of the usual quantity $\Delta_L(p,\Omega)$ the jump $[\alpha']$ can be written (see Appendix) as

$$\mathrm{Im}(\Delta_L(p,\Omega))=[r\alpha']. \tag{14}$$

Thus introducing the flux function $\psi=rb_r$, and making use of the large aspect ratio expansion $m^2\gg k^2r^2$, the toroidal electromagnetic torque acting on the plasma at the mode rational surface is given by

$$\begin{aligned}T_\phi(r_s)=&-2\pi^2R_0n/m^2(|\psi(r_s)|^2e^{2\gamma t}\,\mathrm{Im}[\Delta_L(p+i\Omega)]\\ &+|\hat{\psi}(r_s)|^2\,\mathrm{Im}[\Delta_L(i\Omega)]).\end{aligned} \tag{15}$$

A more useful form of the torque is obtained by expressing it in terms of $\psi(r_w)$ (for the RWM) and $\hat{\psi}_{\mathrm{vac}}$ (for the

error field). This can be achieved by noting that the RWM and the error field independently satisfy torque balance, so that

$$|\psi(r_s)|^2(\omega-\Omega)\tau_L=|\psi(r_w)|^2\omega\tau_w, \tag{16}$$

$$|\hat{\psi}(r_s)|^2\Omega\tau_L=mI\,\mathrm{Re}[\hat{\psi}(r_w)] \tag{17}$$

$$=|\hat{\psi}_{\mathrm{vac}}|^2m^2\frac{\Omega\tau_L(1-\epsilon\delta)}{1+\epsilon^2\Omega^2\tau_L^2}, \tag{18}$$

and we finally obtain the torque at r_s in the form

$$T_\phi(r_s)=-2\pi^2R_0n/m^2\left(|\psi(r_w)|^2e^{2\gamma t}\omega\tau_w+|\hat{\psi}_{\mathrm{vac}}|^2m^2(1-\epsilon\delta)\frac{\Omega\tau_L}{1+\epsilon^2\Omega^2\tau_L^2}\right). \tag{19}$$

VI. TOROIDAL MOMENTUM BALANCE

In this section we follow the treatment by Fitzpatrick.[18] We define $\Omega(r)$ as the toroidal rotation in the presence of error fields and a growing RWM, $\Omega_0(r)$ as the rotation in the absence of the RWM and $\hat{\Omega}_0(r)$ as the toroidal rotation which would be found in the absence of both RWM and error fields and assume that the equilibrium evolution is slow and that RWM growth is slow enough that quasistationary solutions of the momentum equation are valid. Then, in the presence of a momentum source function $S_0(r)$, $\hat{\Omega}_0$, Ω_0, and Ω satisfy the following diffusion equations:

$$S_0+\frac{1}{r}\frac{d}{dr}\left(r\mu\frac{d\hat{\Omega}_0}{dr}\right)=0, \tag{20}$$

$$S_0+\frac{1}{r}\frac{d}{dr}\left(r\mu\frac{d\Omega_0}{dr}\right)=\langle[\hat{j}\times\hat{b}]/R\rangle, \tag{21}$$

$$S_0+\frac{1}{r}\frac{d}{dr}\left(r\mu\frac{d\Omega}{dr}\right)=\langle[(\hat{j}+j)\times(\hat{b}+b)]/R\rangle, \tag{22}$$

where μ is the (anomalous) perpendicular viscosity and $\langle X\rangle$ denotes the flux surface average of X. Recalling that the error field and RWM torque terms are nonvanishing only at the mode rational surface r_s, differencing these equations to eliminate the source term yields

$$\frac{1}{r}\frac{d}{dr}\left(r\mu\frac{d}{dr}(\Omega_0-\Omega)\right)=0, \tag{23}$$

$$\frac{1}{r}\frac{d}{dr}\left(r\mu\frac{d}{dr}(\hat{\Omega}_0-\Omega)\right)=0 \tag{24}$$

at all radii except at r_s. Now assuming that μ is constant, for simplicity, these equations can be solved separately in the intervals $[0,r_s]$ and $[r_s,a]$, making use of the boundary conditions $\hat{\Omega}_0'(0)=\Omega_0'(0)=\Omega'(0)=0$ and $\hat{\Omega}_0(a)=\Omega_0(a)=\Omega(a)=0$, to find

$$\frac{[r(\Omega_0'-\Omega')]}{(\Omega_0-\Omega)}=\frac{1}{\log(r_s/a)}, \tag{25}$$

$$\frac{[r(\hat{\Omega}_0'-\Omega')]}{(\hat{\Omega}_0-\Omega)}=\frac{1}{\log(r_s/a)}, \tag{26}$$

where, as before, we use the notation $[X']=(X'(r_s+)-X'(r_s-))$: i.e., we obtain jump conditions for these functions. Now, returning to Eqs. (20), (21), (22) and integrating them across the mode rational surface $r=r_s$, where the electromagnetic torques appear, we obtain the three equations:

$$4\pi^2R_0^3\mu[r\hat{\Omega}_0']=0, \tag{27}$$

$$4\pi^2R_0^3\mu[r\Omega_0']=\hat{T}_\phi(\Omega_0), \tag{28}$$

$$4\pi^2R_0^3\mu[r\Omega']=\hat{T}_\phi(\Omega)+T_\phi(\Omega). \tag{29}$$

Finally the jump conditions [Eqs. (25) and (26)] allow us to replace the jumps $[r(\Omega_0'-\Omega')]$ by the values $(\Omega_0-\Omega)$ evaluated at r_s. Thus we finally obtain algebraic equations for the plasma rotation $\Omega(r_s)$ at the resonant surface in the presence of both error fields and a growing RWM,

$$(\Omega_0-\Omega)\tau_L=C_{\mathrm{rwm}}\omega\tau_w+C_{\mathrm{err}}(1-\epsilon\delta)\times\left(\frac{\Omega\tau_L}{1+\epsilon^2\Omega^2\tau_L^2}-\frac{\Omega_0\tau_L}{1+\epsilon^2\Omega_0^2\tau_L^2}\right), \tag{30}$$

$$(\hat{\Omega}_0-\Omega)\tau_L=C_{\mathrm{rwm}}\omega\tau_w+C_{\mathrm{err}}(1-\epsilon\delta)\left(\frac{\Omega\tau_L}{1+\epsilon^2\Omega^2\tau_L^2}\right), \tag{31}$$

where

$$C_{\mathrm{rwm}}=e^{2\gamma t}|\psi(r_w)|^2\frac{n\,\mathrm{Log}[a/r_s]}{2m^2\mu R_0^2}\tau_L, \tag{32}$$

$$C_{\mathrm{err}}=|\psi_{\mathrm{vac}}|^2\frac{n\,\mathrm{Log}[a/r_s]}{2\mu R_0^2}\tau_L \tag{33}$$

are dimensionless measures of the RWM amplitude and the error field amplitude, respectively, and $\omega=\omega(\Omega)$ and $\gamma=\gamma(\Omega)$ are the frequency and growth rate of the RWM and must be obtained by solution of the RWM dispersion relation.

VII. NUMERICAL VALUES FOR C_{rwm} AND C_{err}

In the preceding section we derived equations to calculate the evolution of the toroidal plasma rotation $\Omega(r_s)$ under the influence of torques generated by a growing resistive wall mode and an error field whose amplification may be changing. The quantities C_{rwm} and C_{err} control the magnitude of these effects. Noting that

$$C_{\mathrm{rwm}}\sim\frac{\rho a^2\tau_L}{\mu}\frac{B^2}{\rho R_0^2}\frac{b^2}{B^2}\frac{1}{2}\mathrm{Log}[a/r_s] \tag{34}$$

$$\sim\frac{1}{10}\frac{\tau_V\tau_L}{\tau_A^2}\frac{b^2}{B^2}, \tag{35}$$

where τ_V is the momentum confinement time and τ_A the Alfvén time. We can estimate the value of C_{rwm} for a linearly growing RWM emerging from the background electromagnetic noise by taking

$$\frac{b}{B}\sim 10^{-4}, \quad \frac{\tau_V}{\tau_A}\sim \frac{10^{-1}s}{10^{-7}s}\sim 10^6, \quad \frac{\tau_L}{\tau_A}\sim 10^2. \tag{36}$$

so that $C_{\mathrm{rwm}}\sim 10^{-1}e^{2\gamma t}$ as the RWM begins to grow. Similar estimates for the error fields, assuming

$$\frac{\hat{b}}{B}\sim \frac{10G}{3\times 10^4 G}\sim 3\times 10^{-4}, \tag{37}$$

yield values of $C_{\mathrm{err}}\sim 1$. We make use of these estimates in choosing numerical values for C_{rwm} and C_{err} in the following sections.

To recap, we have defined

(i) $\hat{\Omega}_0$ as the plasma rotation frequency that would occur in the absence of both the error field and the RWM.
(ii) Ω_0 as the rotation in the absence of the RWM, but in the presence of the error field.
(iii) Ω as the rotation that occurs in the presence of both the RWM and the error field.

Accordingly, the torque balance at the internal resonance can be expressed as

$$(\Omega_0-\Omega)\tau_L = C_{\mathrm{rwm}}\omega\tau_w + C_{\mathrm{err}}(1-\epsilon\delta)\left[\frac{\Omega\tau_L}{1+\epsilon^2\Omega^2\tau_L^2} - \frac{\Omega_0\tau_L}{1+\epsilon^2\Omega_0^2\tau_L^2}\right] \tag{38}$$

or, equivalently

$$(\hat{\Omega}_0-\Omega)\tau_L = C_{\mathrm{rwm}}\omega\tau_w + C_{\mathrm{err}}(1-\epsilon\delta)\frac{\Omega\tau_L}{1+\epsilon^2\Omega^2\tau_L^2}, \tag{39}$$

where C_{rwm} and C_{err} are normalized expressions of the RWM and error field amplitudes.

VIII. THE EFFECT OF COMBINED ERROR FIELD AND RWM TORQUES

We are now in a position to investigate the effect of the RWM and/or the error field on the plasma torque balance. The natural expression to use is Eq. (39), as this will be the most germane to actual experimental observations. As remarked above, Fig. 1 shows the evolution of the plasma rotation in the absence of any error field (i.e., $C_{\mathrm{err}}=0$) against a growing C_{rwm}, exhibiting the well-known S-curve behavior. As described in Ref. 8 this set of curves can well be proposed as an explanation for the experimentally observed behavior of the RWM growth and plasma rotation evolution in DIII-D (Fig. 2). In Fig. 1, and all subsequent graphs, a typical set of parameters for the RWM were chosen: namely, $\epsilon=0.01$, $\delta=0.5$; it is also assumed that the ratio of plasma layer time to wall time is unity (see Discussion and Conclusions section).

To interpret the content of the S-curves in Fig. 1 (and later figures) it is convenient to visualize a time dependent scenario in which C_{rwm} is slowly growing. Each member of the family of S-curves in Fig. 1 then represents the resulting evolution of the rotation $\Omega(r_s,t)$ of an equilibrium as it progresses through a set of quasistatic states with decreasing rotation: i.e., decreasing Ω in response to the increasing torque, which is proportional to C_{rwm}. Considering the top trajectory of the family (with $\Omega=10$ for $C_{\mathrm{rwm}}=0$), the S-curve shows that an equilibrium which has evolved continuously from $\Omega=10$ when $C_{\mathrm{rwm}}=0$, to reach the state labeled A in Fig. 1 must experience a jump to the remote new state, labeled B, with a much lower value of rotation Ω, when $C_{\mathrm{rwm}}>25$. In Ref. 8 it was suggested that it was an equilibrium transition of this type which might give rise to a rapid acceleration of the growth of a pre-existing RWM. However, the point made in Ref. 19 is that similar behavior might be expected when only an error field is present. This is indeed a possibility. The evolution of $\Omega(r_s,t)$ must then be driven, not by an increase in C_{err}, which is fixed, but by the evolution of the equilibrium towards an instability threshold for a kink mode (or a tearing mode), as $\epsilon(t)$ varies. As this happens, the error field amplification increases, and with it the torque. The result should be a reduction of the plasma rotation rate, and the possible triggering of an RWM if $\Omega(r_s)$ falls below a critical value. In this scenario[19] elimination of the resonant error field is all that is required to maintain RWM stability.

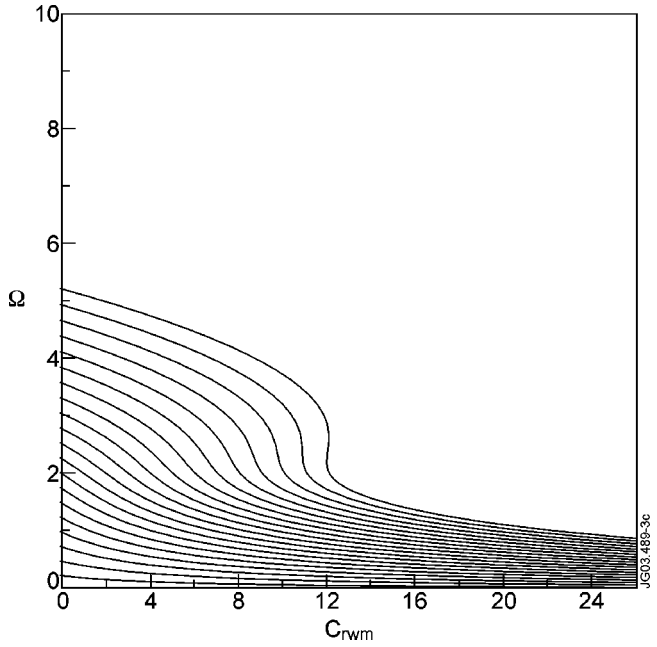

FIG. 3. Rotation as a function of C_{rwm}, with the same parameters as in Fig. 1, but with the introduction of some error coil current.

Since the suggestions of Refs. 8 and 19, DIII-D have demonstrated[15] that the presence or absence of an error field can significantly affect the duration of an AT discharge (see Fig. 6). This may be a possible explanation of why the original S-curves of Ref. 8 were referred to as "qualitatively, but apparently not quantitatively, correct."

So, first we examine solutions to Eq. (39) (which, with the absence of C_{err} yields Fig. 1) in the presence of a fixed nonzero error field C_{err}. The result is shown in Fig. 3. These curves of plasma rotation rates against C_{rwm} have exactly the same initial momentum drive ($C_{\mathrm{rwm}}=0$) as those of Fig. 1, and so we see immediately by comparing the two figures that

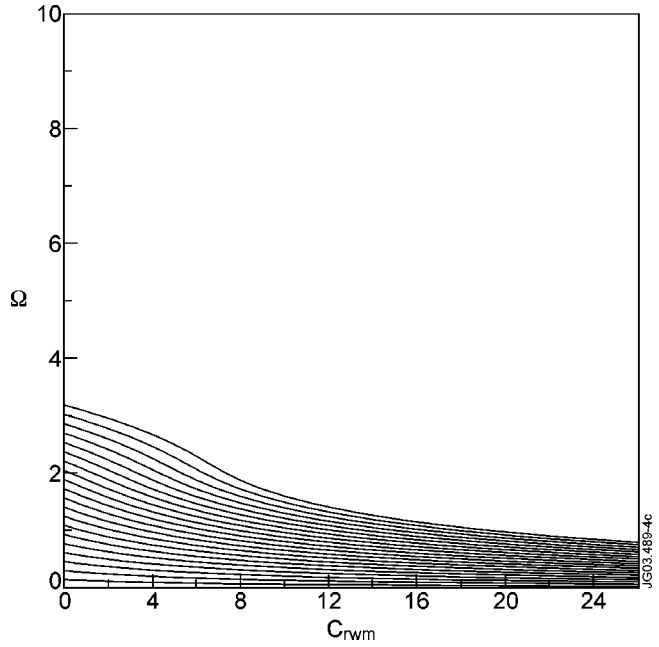

FIG. 4. The same parameters as Figs. 1 and 3, with further error field coil current.

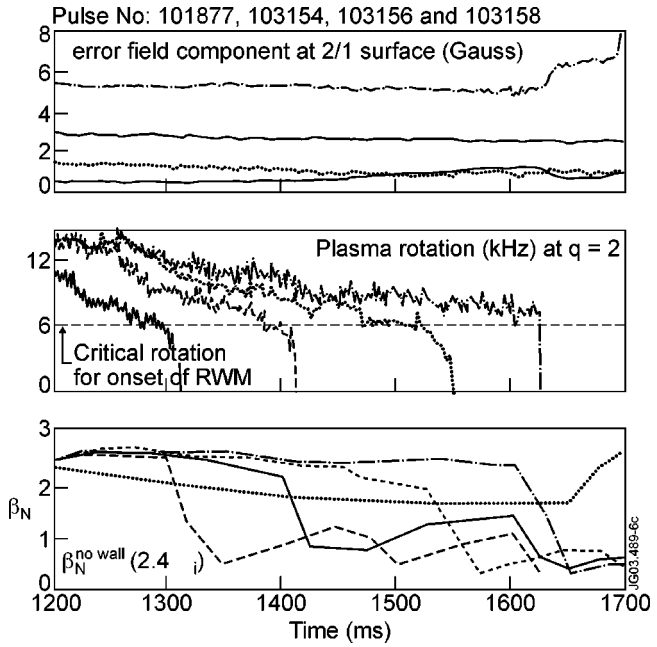

FIG. 6. DIII-D observations of the effect of decreasing the error field by means of externally applied coil currents.

the error field has a braking effect on the initial plasma rotation (the difference between $\hat{\Omega}_0$ and Ω_0). This in itself is not surprising and has been investigated by many authors (see, e.g., Ref. 21). A further increase in the error field amplitudes leads to Fig. 4 and we see that for the same initial drives the *S*-curve behavior has completely disappeared.

However, if we increase the range of initial drives we arrive at Fig. 5, and clearly, this figure indicates that the presence of an error field does not basically change the topology of the *S*-curves, but can significantly change the parameter regime in which it occurs—bringing about a possible reconciliation with the DIII-D quantitative results.

The final result we have generated from the torque balance given by Eq. (39) is an attempt to simulate the observations (see Fig. 6) that a reduction in error field amplitude leads to a longer duration of the discharge when it is above the RWM β limit. In order to reproduce Fig. 6 we have to translate C_{rwm} into actual time. Assuming that C_{rwm} grows exponentionally, then taking the natural logarithm of Eq. (39) to reconstruct time variation leads to Fig. 7. This figure is a

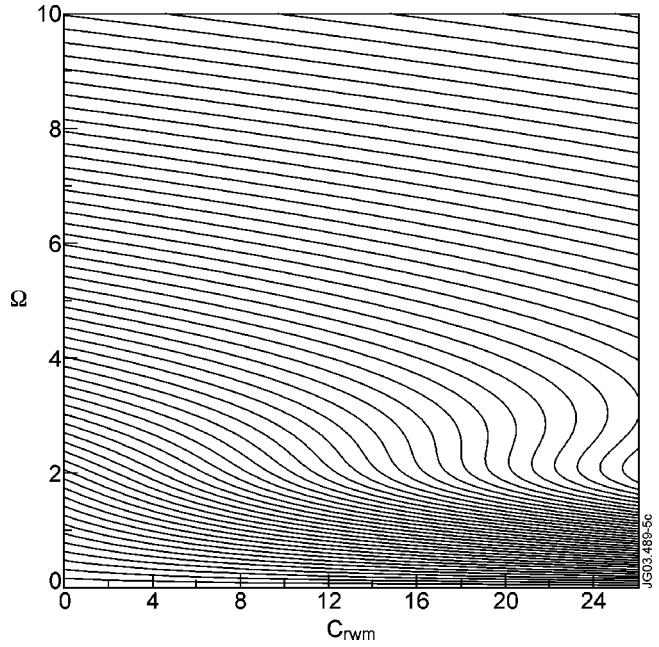

FIG. 5. Same as Fig. 3 with extended range of parameters (i.e., larger initial momentum drive).

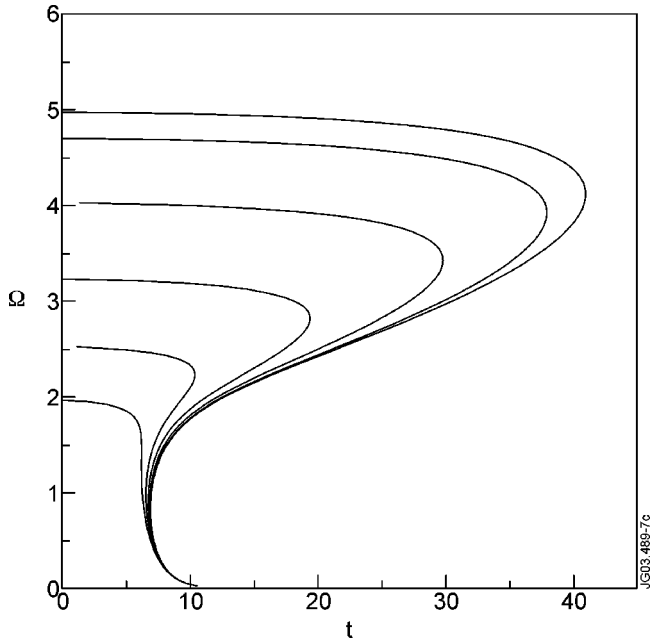

FIG. 7. Simulation of rotation rate against time with decreasing amount of error field coil current. The lowest curve (starting at $\Omega_0 \sim 2.0$) represents the largest error field, and the highest curve ($\Omega_0 \sim 5$) represents zero error field.

plot of Ω_{r_s} against time for decreasing amounts of error field amplitude (the curves extend to the right as the error field is reduced). Clearly, reducing the error field coil current C_{err} has a similar effect in increasing the duration of the discharge with a RWM present. Further, the extension of the discharge duration appears to be comparable, in ratio, between Figs. 6 and 7. The lowest curve in Fig. 7 (starting at $\Omega_0 \sim 2.0$) represents the largest error field, and the highest ($\Omega_0 \sim 5$) represents zero error field, clearly showing the extension of discharge duration.

IX. DISCUSSION AND CONCLUSIONS

We have reviewed the present state of theoretical understanding of the effect that the presence of an error field has on the growth of a resistive wall mode (RWM).[18,19] This review included a discussion of the notion of error field amplification when RWM marginal stability was approached, and it was pointed out that it is the current generating the error field that is the fixed quantity in this calculation, *not* the resulting error field flux, which is essentially an eigenvalue of the calculation. The central point in this work is that of the effect of plasma rotation on the RWM. As we have pointed out, this depends on the details of the internal plasma dynamics. In the model we have used (with internal mode resonance[9] and visco-resistive layer dynamics) the RWM cannot be stabilized by plasma rotation at values of β_N above the no-wall β limit. If this model is applicable to ITER,[1] steady state operation above the no-wall β limit in AT operation would require active feedback stabilization of the RWM[22,23] or passive stabilization (e.g., by a secondary rotating wall[24,25] or by a more complex moving wall such as the Zakharov flowing wall concept provides[26]). Fitzpatrick[18] has, however, constructed an alternative plasma model in which rotational stabilization of the RWM above the no-wall β limit is possible [i.e., a model showing type (c) behavior, rather than type (b) behavior, as discussed in the Introduction]. Boozer[19] does not make use of any specific plasma model, but inherently assumes type (c) behavior: i.e., that rotational stabilization of the RWM is possible. Boozer has drawn attention to the importance of the error fields and points out that the observations on DIII-D[14] can be interpreted in terms of error field amplification and a rotation threshold for the RWM [type (c) behavior]. However, in our foregoing analysis using torque balance we have produced a simulation (Fig. 7) of the DIII-D result[14] showing that a reduction in error field amplitude leads to an increase in discharge duration. This suggests that the experimental results on DIII-D do not definitively confirm that rotational stabilization of the RWM is possible. As we have pointed out there may also be some confusion between the resistive wall *tearing* mode (RWTM), which is stabilised by modest plasma rotation, and the ideal RWM, which (in our model) is not. We conclude that, because of the continuing uncertainty in what internal plasma dynamics actually determines RWM behavior, it is not yet possible to predict, with conviction, whether steady state operation of an advanced tokamak scenario in ITER[1] will be possible without active feedback control. Detailed comparison of experimental data from current large tokamak devices, with the predictions from alternative plasma models (such as the Fitzpatrick–Aydemir model, our visco-resistive Finn model, and others) is required and future experiments may resolve this issue.

ACKNOWLEDGMENTS

We gratefully acknowledge illuminating discussions with Alan Boozer.

This work was funded jointly by the United Kingdom Engineering and Physical Sciences Research Council and by EURATOM.

APPENDIX: RELATION BETWEEN $\mathrm{Im}(\Delta_L)$ AND $[r\alpha']$

In Sec. V, representing the magnetic perturbations in terms of real quantities with

$$\tilde{b}_r = e^{\gamma t} b_r(r)\cos(\xi+\alpha),$$

$$\tilde{b}_\theta = e^{\gamma t}(b_{\theta c}(r)\cos(\xi+\alpha) + b_{\theta s}(r)\sin(\xi+\alpha),$$

$$\tilde{b}_\phi = e^{\gamma t}(b_{\phi c}(r)\cos(\xi+\alpha) + b_{\phi s}(r)\sin(\xi+\alpha)),$$

where $\xi = (m\theta - n\phi - \omega t)$, we derived an expression relating the local torque to a jump in the derivative of the phase variable α. In previous work, starting from a complex representation of the perturbing fields in the form

$$\tilde{\mathbf{b}} = \mathbf{b} e^{i\xi+\gamma t}$$

Fitzpatrick[22] related the torque to the imaginary part of the (complex) jump $\Delta_L(p+i\Omega)$ across the resonant layer. Here we demonstrate the equivalence of these results. Starting with the complex representation

$$\tilde{b}_r = \mathrm{Re}(b_r e^{i\xi+\gamma t}) = e^{\gamma t}(\mathrm{Re}(b_r)\cos(\xi+\alpha) - \mathrm{Im}(b_r)\sin(\xi+\alpha)),$$

where

$$\frac{\mathrm{Im}(b_r)}{\mathrm{Re}(b_r)} = \tan(\alpha),$$

and using the definition of $\Delta_L = [rb_r']/b_r$ we obtain

$$\mathrm{Im}(\Delta_L) = \frac{(\mathrm{Re}(b_r)\mathrm{Im}[rb_r'] - \mathrm{Im}(b_r)\mathrm{Re}[rb_r'])}{|b_r|^2}.$$

Now using,

$$\mathrm{Re}(b_r) = |b_r|\cos(\alpha),$$

$$\mathrm{Im}(b_r) = |b_r|\sin(\alpha),$$

$$\mathrm{Re}(rb_r') = r|b_r'|\cos(\alpha) - r\alpha'|b_r|\sin(\alpha),$$

$$\mathrm{Im}(rb_r') = r|b_r'|\sin(\alpha) + r\alpha'|b_r|\cos(\alpha),$$

one finds

$$\mathrm{Im}(\Delta_L) = [r\alpha'].$$

[1]ITER Physica Basis, Nucl. Fusion **39**, 2175 (1999).
[2]C. E. Kessel, J. Manickam, G. Rewoldt, and W. M. Tang, Phys. Rev. Lett. **72**, 1212 (1994).
[3]J. Manickam, M. S. Chance, S. C. Jardin *et al.*, Phys. Plasmas **1**, 1601 (1994).
[4]A. Bondeson, M. Benda, M. Persson, and M. S. Chu, Nucl. Fusion **37**, 1419 (1997).
[5]C. G. Gimblett, Nucl. Fusion **26**, 617 (1986).
[6]B. Alper, M. K. Bevir, H. A. B. Bodin *et al.*, Plasma Phys. Controlled Fusion **31**, 205 (1989).
[7]P. Greene and S. Robertson, Phys. Fluids B **5**, 556 (1993).
[8]C. G. Gimblett and R. J. Hastie, Phys. Plasmas **7**, 258 (2000).
[9]J. M. Finn, Phys. Plasmas **2**, 198 (1995); **2**, 3782 (1995).
[10]H. P. Furth, J. Killeen, and M. N. Rosenbluth, Phys. Fluids **6**, 459 (1963).
[11]R. Fitzpatrick, Phys. Plasmas **1**, 3308 (1994).
[12]A. Bondeson and D. J. Ward, Phys. Rev. Lett. **72**, 2709 (1994).
[13]R. Betti and J. P. Friedberg, Phys. Rev. Lett. **74**, 2949 (1995).
[14]A. M. Garofalo, A. D. Turnbull, M. E. Austin *et al.*, Phys. Rev. Lett. **82**, 3811 (1999).
[15]A. M. Garofalo, E. J. Strait, J. M. Bialek *et al.*, Nucl. Fusion **40**, 1491 (2000).
[16]A. M. Garofalo, M. S. Chu, E. D. Fredrickson *et al.*, Nucl. Fusion **41**, 1171 (2001).
[17]A. M. Garofalo, T. H. Jensen, L. C. Johnson *et al.*, Phys. Plasmas **9**, 1997 (2002).
[18]R. Fitzpatrick, Phys. Plasmas **9**, 3459 (2002).
[19]A. H. Boozer, Phys. Rev. Lett. **86**, 5059 (2001).
[20]R. Fitzpatrick and A. Y. Aydemir, Nucl. Fusion **36**, 11 (1996).
[21]D. A. Gates and T. C. Hender, Nucl. Fusion **36**, 273 (1996).
[22]R. Fitzpatrick, Phys. Plasmas **4**, 2519 (1997).
[23]A. Bondeson, Y. Q. Liu, D. Gregoratto, C. M. Fransson, B. Lennartson, C. Brietholtz, Y. Gribov, and V. D. Pustovitov, Phys. Plasmas **9**, 2044 (2002).
[24]C. G. Gimblett, Plasma Phys. Controlled Fusion **31**, 2183 (1989); C. G. Gimblett and R. J. Hastie, Phys. Plasmas **7**, 5007 (2000).
[25]An experiment along these lines is currently being constructed at the University of Wisconsin–Madison.
[26]J. B. Taylor, J. W. Connor, C. G. Gimblett, H. R. Wilson, and R. J. Hastie, Phys. Plasmas **8**, 4062 (2001).